Sensors and Materials, Vol. 37, No. 1 (2025) 155–171
MYU Tokyo

S & M 3898

Semantically Enriched Interpretation for Landslide/Mudslide Susceptibility with Multimodal Remote Sensing Datasets

Zhiyong Ma,[1,3] Yao Feng,[2] Xinguo Guo,[2] Yingwei Zhang,[2] Long Zhang,[2] Quan Yuan,[2] and Chong Niu[1,2*]

[1]School of Environment Science and Spatial Informatics, China University of Mining and Technology, Tongshan District, Xuzhou 221116, China
[2]Shandong GEO-Surveying & Mapping Institute, Lixia District, Jinan 250013, China
[3]Chinese Society for Geodesy Photogrammetry and Cartography, Beijing 100830, China

(Received June 20, 2024; accepted January 9, 2025)

Keywords: landslide/mudslide susceptibility detection, geosemantics, SAR, optical remote sensing, DEM

Landslide/mudslide susceptibility is of significance to socioeconomic sustainable development and emergence management. Although remote sensing datasets have been used for landslide/mudslide susceptibility interpretations, the results might be weak owing to the limitations of the single-modal remote sensing dataset. Evolving Earth observation techniques enable the automatic identification of landslide/mudslide susceptibility over a large extent from multimodal remote sensing datasets. This also poses a major challenge in effective organization, representation, and modeling for complex information on landslide/mudslide susceptibility. In this study, we propose a geospatial semantic model to formally represent the interpretation of visual features from optical remote sensing, deformation features from synthetic-aperture radar (SAR) datasets, terrain features from digital elevation models (DEMs), and descriptions by field investigations. First, we applied optical remote sensing image, DEM, and SAR datasets to detect and annotate the features of landslide/mudslide susceptibility. Then, we developed a geospatial ontology to represent these features in a machine-understandable format. Depending on the triple structure of "domain-property-range" and the rules and restriction set by the proposed geospatial ontology, we created a semantic model to conduct semantic query and reasoning for landslide/mudslide susceptibility. The proposed semantic model for landslide/mudslide susceptibility interpretation has been successfully tested in four counties in Yunnan Province, China. We expect this work to be a major contribution to the integration of knowledge from both remote sensing and GIS data, and to deepen the application of semantic web technology in landslide/mudslide susceptibility domains.

*Corresponding author: e-mail: niuchong@cumt.edu.cn
https://doi.org/10.18494/SAM5190

ISSN 0914-4935
https://myukk.org/

1. Introduction

Landslide/mudslide susceptibility assessment, also known as sensitivity assessment, forms the basis of landslide/mudslide risk and hazard assessments.[1,2] It allows the evaluation of the effects and contributions of various factors to the occurrence of hazards under certain environmental conditions and the determination of the tendency and likelihood of landslide/mudslide occurrence through comprehensive analysis.[3] The evaluation results are then combined with the development characteristics of landslides and mudslides to divide the region into different levels, with a relative emphasis on revealing the spatial distribution of hazard points.

Optical remote sensing interpretation is one of the main methods that currently utilize the multispectral information about the object for conducting an early interpretation of landslide hazards.[4] In landslide/mudslide research, high spatial and spectral resolutions are used to enhance and extract optical image information by various image processing techniques and spectral relevant information to identify landslide features. This requires remote sensing imagery. However, it is considerably affected by clouds and fog, and often can only provide a qualitative interpretation of large-scale landform features.

As an emerging technology in the past three decades, Interferometric Synthetic Aperture Radar (InSAR) has specific advantages such as all-weather capability, continuous monitoring, and certain penetration ability. It is suitable for conducting large-scale landslide/mudslide surveys and the long-term monitoring of small deformations, which have been widely used in various fields such as terrain measurement, geological exploration, disaster prevention and mitigation, and agricultural, forestry, and marine research. InSAR can extract terrain information using the phase information of radar images. Differential InSAR (D-InSAR) technology enables the measurement of small deformations on Earth's surface, which promotes the development of interferometric measurement techniques.[5] The D-InSAR deformation extraction results are highly consistent with conventional ground monitoring results. In addition, interferometric measurement might be invulnerable to the coherence loss in dense vegetation areas, meaning that differential interferometric measurement technology is suitable for monitoring small-scale surface deformations.[6–9]

Single remote sensing sensors are constrained by various types of weather and terrain, making them available for accurately acquiring the data that we need. In recent years, the rapid development of multiplatform remote sensing measurement technology has provided important technical means for landslide/mudslide risk assessment.[10,11] The available platforms include satellite platforms for optical and SAR remote sensing, and airborne and unmanned aerial vehicle (UAV) platforms for optical remote sensing and LiDAR.[12] These systems enabled the interpretation and monitoring of major landslide/mudslide risks from multiple dimensions and scales, addressing the challenges of "where are the hidden risks" and "when they may occur".[13]

Multimodal remote sensing is of significance to efficient landslide/mudslide susceptibility prediction.[14] Moreover, since the determination of systematic mechanisms, that is, reagreeing clues of landslides and mudslides are difficult to define using statistical features learned in deep

learning techniques, semantics and a knowledge graph can be transformed into explainable clues for landslide/mudslide susceptibility prediction.[15] Thus, in this paper, we report our efforts on developing a semantically enriched dataset for landslide/mudslide susceptibility with multimodal remote sensing datasets.

This manuscript is organized as follows. In Sect. 2, we discuss the previous works related to landslide/mudslide susceptibility using different types of remote sensing dataset. In Sect. 3, we present the details of the developed semantically enriched datasets, including architecture, interpretation routines, and semantic modeling approaches. In Sect. 4, we illustrate the implementations of the semantically enriched datasets. In Sect. 5, we summarize the highlights of our contributions for landslide/mudslide susceptibility interpretation.

2. Related Works

2.1 Digital elevation model (DEM)-based landslide/mudslide susceptibility prediction

Geohazard interpretation enhanced by DEMs can use other diagnostic features of the hazards such as terrain and texture, yielding significantly better results than methods solely relying on image spectral features. The automated interpretation of landslides, which incorporates multiple information sources, including DEMs, can generally be accomplished with the support of a GIS system, which supports the extraction of terrain information such as slope and aspect, and the conduct of composite analysis.[16] Similarly, Iwahashi *et al.*[15] utilized DEMs to extract information such as terrain slope, terrain texture, and local convexity, enabling the automatic classification of the terrain and laying the foundation for further automated landslide interpretation. Zhou *et al.*[17] proposed the establishment of a spatial disaster information system using network database technology, GIS, and remote sensing techniques, successfully applied to the investigation, assessment, and prediction of debris flows, landslides, and other disasters.

2.2 Optical remote-sensing-based landslide/mudslide susceptibility prediction

Remote sensing can realistically display the morphological, tonal, and textural features of landslides and the boundary characteristics, scale, shape, and breeding environment of landslide hazards. Thus, landslide remote sensing investigations often combine satellite and aerial photography techniques for observing the spatial distribution and relationship between landslides and mudslides, and regional topography, geological structures, and other factors. These factors are used for studying the characteristics of hazards and exploring their overall occurrence trends.

The application of remote sensing technology in landslide investigations can be traced back to the late 1970s when aerial remote sensing images were compiled as a 1:50,000-scale national landslide/mudslide distribution map. Many scholars conducted landslide research using remote sensing technology, including landslide detection, interpretation, and classification, landslide activity monitoring, and landslide hazard analysis.[19,20]

Recently, the development of remote sensing technology has provided more methods for landslide hazard interpretation. The systematic research on existing landslides within the target area and optical remote sensing technology in landslide/mudslide investigations have gradually evolved from simple remote sensing data to comprehensive analysis methods involving multiple temporal phases and data sources. Marcelino *et al.*[20] used different fusion methods to fuse ETM+ and SPOT panchromatic images to obtain landslide data. The results showed that the IHS fusion technique best preserved the spatial and spectral information of the original images, enabling a clearer interpretation of landslide traces.

2.3 SAR-based landslide/mudslide susceptibility prediction

Singleton *et al.*[5] demonstrated the effective use of D-InSAR for monitoring small-scale sliding deformations in a specific area. Subsequently, scholars conducted research on the application of D-InSAR in landslide monitoring and achieved many successful results.[7] However, for mountainous areas with significant terrain variations, satellite-borne InSAR is often constrained by factors such as geometric distortion, temporal and spatial decorrelations, and atmospheric disturbances. These limitations result in a large number of unrelated signals or the absence of deformation information in the interferogram.[8] Additionally, the deformation phase obtained by InSAR often includes atmospheric delay, which affects the accuracy of surface deformation measurement.

Ferretti *et al.* proposed the concept of permanent scatterers (PS) for handling multiple radar images acquired at different times.[7] The PS-InSAR method selects temporally stable strong reflectors, namely, PS, for processing local image regions instead of the entire image.[22] The selection of stable and minimally deforming PS points avoids unwrapping errors caused by large deformations and improves the deformation measurement accuracy. Berardino *et al.*[22] proposed another method called the small baseline subset (SBAS) method.[23] This method restricts the temporal and spatial baselines to ensure the coherence of the interferogram, and it can process selected points or the entire image as needed.[24] It performs interferometry on single-look complex (SLC) images with temporal and spatial baselines within a certain reliable range. PS-InSAR and SBAS-InSAR techniques reduce the effects of temporal and spatial decorrelations and atmospheric delay for the early interpretation of landslide hazards, which are limitations of traditional InSAR and D-InSAR measurement methods. These techniques produce surface deformation results with better temporal and spatial continuities and higher accuracy for improving the dynamic monitoring and early interpretation of landslides/mudslides.[25,26] These successful cases demonstrate the advantages of time-series InSAR technology in extracting information on broad-scale geological deformations, providing important technical means for the investigation and study of landslide/mudslide risks.

3. Semantic Interpretation

3.1 Architecture

Figure 1 presents the architecture of a semantically enriched dataset, which includes five classes: Attributes, Visual Conditions, Geological Conditions, Deformation Conditions, and Field Investigations. Attributes record the meta-information regarding each landslide/mudslide susceptibility point. Visual Conditions record the visual interpretation results from optical remote sensing datasets. Deformation Conditions record the In-SAR interpretation results. Geological Conditions record the terrain features derived from DEMs, and Field Investigations record the results generated by field investigations.

Moreover, Fig. 2 presents the workflow of developing the semantically enriched dataset, which includes four parts: field investigation, data interpretation, semantic modeling, and semantically enriched dataset function.

Geographical coordinates can be accessed from multimodal remote sensing datasets. Field investigation determines the geographical names for the place that corresponds to the geographical coordinates. Moreover, field investigation provides auxiliary attributes inaccessible from multimodal remote sensing datasets.

Data interpretation includes the visual features generated from optical remote sensing images, the terrain features generated from DEMs, and the deformation features derived from SAR datasets.

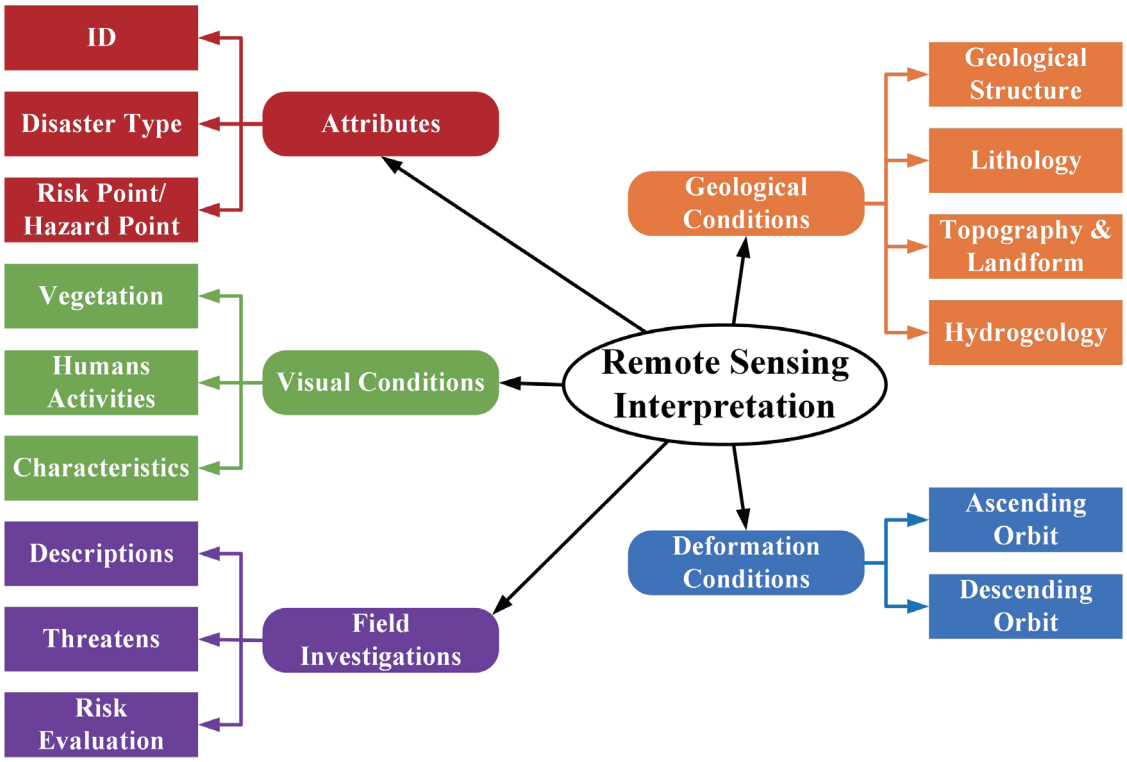

Fig. 1. (Color online) Architecture of remote sensing interpretation for landslide/mudslide susceptibility.

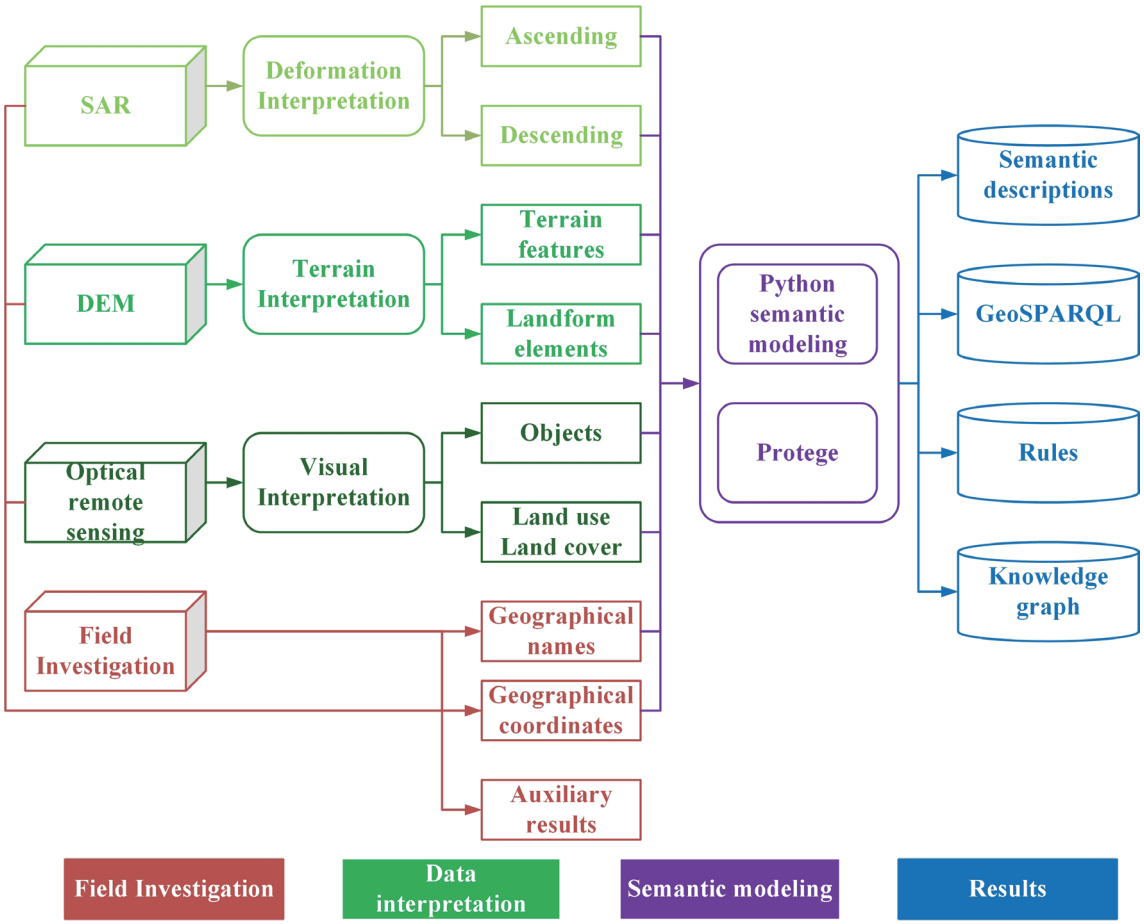

Fig. 2. (Color online) Workflow of semantic modeling of topographic features.

Semantic modeling explicitly defines the features by creating an ontology, including classes, individuals, and properties. On the basis of the ontology, we developed semantic descriptions on the basis of W3C Semantic Web standards, a GeoSPARQL defined by the Open Geospatial Consortium (OGC) for semantic query, rules for domain logic reasoning, and the knowledge graphs created on the basis of rules.

3.2 Data interpretation

3.2.1 Visual interpretation for optical remote sensing dataset

Visual interpretation primarily relies on the direct interpretive features of geological disasters, such as color tone, shape, and texture. These features are combined with comprehensive information characteristics, including topography, geology, hydrology, vegetation, and slope to identify and delineate the distribution characteristics of collapses, landslides, and debris flows. The details of field investigation regarding visual interpretation can be found in Ref. 1.

(1) Collapses

Visual interpretation for collapses utilizes the color and texture features of collapse-prone areas. Specifically, in local sections of steep mountains with a steep upper part and a gentle lower part, collapses are identified by the sudden appearance of relatively light color anomalies and rough, rugged textures compared with the surrounding terrain. Moreover, the interpretation method relies on the geological definitions related to collapses occurring in cliffs, steep slopes, or uneven residual rock masses.

(2) Landslides and mudslides

Visual interpretation for landslides utilizes the color and texture features of landslide-prone areas. In local sections of mountains, landslides are identified by the sudden appearance of relatively light color tones, uneven color distribution, fragmented terrain, undulating surface, uneven slope subsidence, and the presence of rough textures and patchy shadow patterns. Moreover, visual interpretation considers the geological definitions related to landslides occurring in gentle slopes of multiple landslide-prone valleys, shaded slopes of dividing ridges, junctions of main and tributary gullies with rapid changes in erosion base levels, and heads of gullies.

Moreover, the distribution range of deformation areas can be determined. Deformation areas always appear lighter or whiter than the surrounding terrain, with rough surface textures, distinct erosion grooves, and local anomalies such as creep, slippage, and stepped faults.

3.2.2 Terrain interpretation for DEM

A DEM is used to extract ridge and valley lines of hilly areas based on the DEM of counties and districts. These ridge and valley lines are used to delineate the distribution range of small watersheds on the basis of the convergence rules of multiple-level water systems. Terrain interpretation for debris flows relies on the geological definitions related to the three zones, namely, source, transport, and deposition areas, clearly visible in the standard channels of debris flows. Source areas exhibit steep slopes, severe rock weathering, and abundant loose materials, appearing as clear anomalies with light color tones, rough textures, and clear signs of rainwater erosion in remote sensing images. Transport areas are characterized by straight or curved gullies with jagged edges and rough textures. Deposition areas are typically located at the exits of valleys, exhibiting flat and open fan-shaped features with relatively light color tones and fine and irregular textures.

3.2.3 Deformation interpretation for satellite SAR dataset

InSAR deformation data in ascending and descending orbits are used to identify and delineate deformation-dense areas. The color-rendered deformation parameters and deformation rates of the surveyed areas are dynamically displayed and analyzed using profile lines to visually show the characteristics of the deformation zones. Then, parameters such as area, location, maximum deformation, minimum deformation, and average deformation rate were extracted for each deformation zone.

For InSAR-based landslide deformation analysis, the focus is on the spatial distribution and magnitude of deformations, supplemented by factors such as slope morphology, elevation, slope, vegetation type, geological properties, and distributions of residential areas. Coherence analysis is conducted to examine the coherence between periods of significant deformation in the time series curves of TS-InSAR-monitored landslide deformations and rainy seasons, earthquakes, and human engineering activities. Then, morphological analysis is performed using a high-precision DEM to display landslide areas with severe deformations.

(1) Collapse

Deformation interpretation relies on high-resolution SAR data with a spotlight imaging mode to detect steep rock faces and large incidence angles (>35°). The choice of wavelength depends on the surface vegetation coverage and deformation magnitude, with high-frequency and short-wavelength SAR data being suitable. The regional distribution of collapses (rock masses) should be correlated with terrain, geology, tectonic activities, and human activities. Then, correlation analysis is conducted between the abnormal deformation of individual collapses (rock masses) and regional seismic activity, precipitation, and human activities.

(2) Landslides and mudslides

The spatial distribution and magnitude of deformations are the primary research focus of landslides and mudslides, which includes factors such as the basin, main channel slope, elevation, slope, vegetation coverage, and geological properties. The interpretation and delineation of debris flow locations and distribution areas are achieved through SAR data that hold long archival times and longer wavelengths. Then, the radar's vertical incidence angle for monitoring the activity of single-channel debris flows is chosen on the basis of the characteristics of the terrain, avoiding radar shadowing and overlapping as much as possible, and the SAR's horizontal incidence direction should be parallel to the direction from the source area to the deposition area.

Specifically, the D-InSAR method is used for areas being covered by low atmospheric interference. Moreover, for rainfall-induced debris flows, a multitemporal interferometric radar measurement method combining SBAS-InSAR and PS-InSAR is employed. The spatial deformation distribution of the debris flow source area and the temporal deformation curves of key locations, slope gradients, and basin areas are analyzed to determine the deformation trends and assess their activity.

3.2.4 Field investigation

The terrain, lithology, geological structures, and meteorological and hydrological factors within the work area provide favorable geological conditions for the formation of landslides and mudslides. Human activities such as deforestation, land clearing, mineral resource development, and infrastructure construction deteriorate the geological environment in the area, leading to the occurrence and development of landslides and mudslides.

This interpretation mainly focuses on the micro-topographic features, geological structures, and lithology related to the occurrence of landslides and mudslides, such as terrain fragmentation,

surface cracks, local collapses, wetlands, and abnormal vegetation. It interprets structures, different types of land use plots, transportation corridors, pipeline facilities, villages, and scattered houses that may be threatened by landslides and mudslides at a larger scale. For features with relevant micro-topographic characteristics, optical patterns of landslide/mudslide potential are extracted by identifying the boundaries of ancient (old) landslides and mudslides or mountain slope boundaries. Table 1 shows the category and accuracy requirements of interpretation by field investigation.

3.3 Semantic modeling

Kavouras and Kokla[27] introduced formal concept analysis into geographic information formalization and integration. The formal expression "object-attribute" that they proposed provides a direct method for cross-domain geographic information modeling. Prasad and Guha[28] integrated semantic annotation into concept naming and semantic categorization simultaneously. They claimed that the true key of semantic modeling requires concept naming and their categorization processing in various facets. The geospatial semantic model includes three parts: semantic triple building, property assignment, and rule and restriction setting.

(1) Semantic triple building. We developed semantic triples for explicitly modeling the results of data interpretation, involving visual interpretation, terrain interpretation, deformation interpretation, and the interpretation of field investigation. The triple expression is object-oriented processing and stored as "domain-property-range".

Semantic triples are created using an open-source software program called Protégé and a semantic python package. These two tools all support the creation of ontologies based on

Table 1
Details and accuracy requirements of interpretation by field investigation.

Category	Details	Accuracy Requirements
Terrain and landforms	Morphology, formation types, and boundaries of various landforms Individual and composite features of micro-topography	Geological bodies with an area greater than 4 mm² and deformed geological bodies with a length greater than 2 cm should be interpreted on the image.
Geological structures	Location, length, and extension direction of faults; Types, scales, lengths, and extension directions of folds Properties and distribution of fractured zones	
Lithology	Referring to existing geological data to determine lithostratigraphy, lithology categories, and bedding conditions	
Land use	Types and current distribution of land use, including forests, vegetation, surface water bodies, cultivated land, steep slopes, towns, etc.	
Human engineering activities	Distribution and stability of engineering activities such as slope cutting, reservoir shores, open-pit mining areas, tailings ponds, and solid waste disposal sites	

Semantic Web languages such as W3C Web Ontology Language (OWL) and Resource Description Framework (RDF). With these two tools, all information regarding data interpretation is semantically modeled through the triple store of RDF: subject-predicate-object. Objects and the value corresponding to each property and subproperties are created as individuals. The relations with the text description are created as object properties, the relations with the value range are created as data properties, and the metadata of the changed object and remote sensing imagery are created as annotation properties.

(2) Property assignment. Property assignment is the transfer of all information (values and text descriptions) of interpretations into the individuals of ontology. Since our ontology is designed on the basis of features of change annotation information in data cube, the information of change annotation can be transformed to the ontology directly.

(3) Rule and restriction settings. Depending on the ontology structure, the rule and restriction settings focus on building reasoning rules and restricted conditions for semantic modeling. For instance, the relation with functional characteristics can only have one range with multiple domains. Rule setting includes a reasoner and reference knowledge from a geospatial reference base. The computation of the reasoner relies on the characteristics of logical and topological relations. The knowledge will be stored as the triple structure "domain-property-range." Restriction uses keywords of text description and value range or value point to set the prerequisite of truth of the triple structure "domain-property-range."

The architecture of the developed ontology is shown in Fig. 3, which consists of two basic groups of vocabulary: Class and Property. Class is used to hierarchically define a diagram for organizing the relationship of each category, which contains Attributes, Visual Conditions, Geological Conditions, and Deformation Conditions, which correspond to the semantically

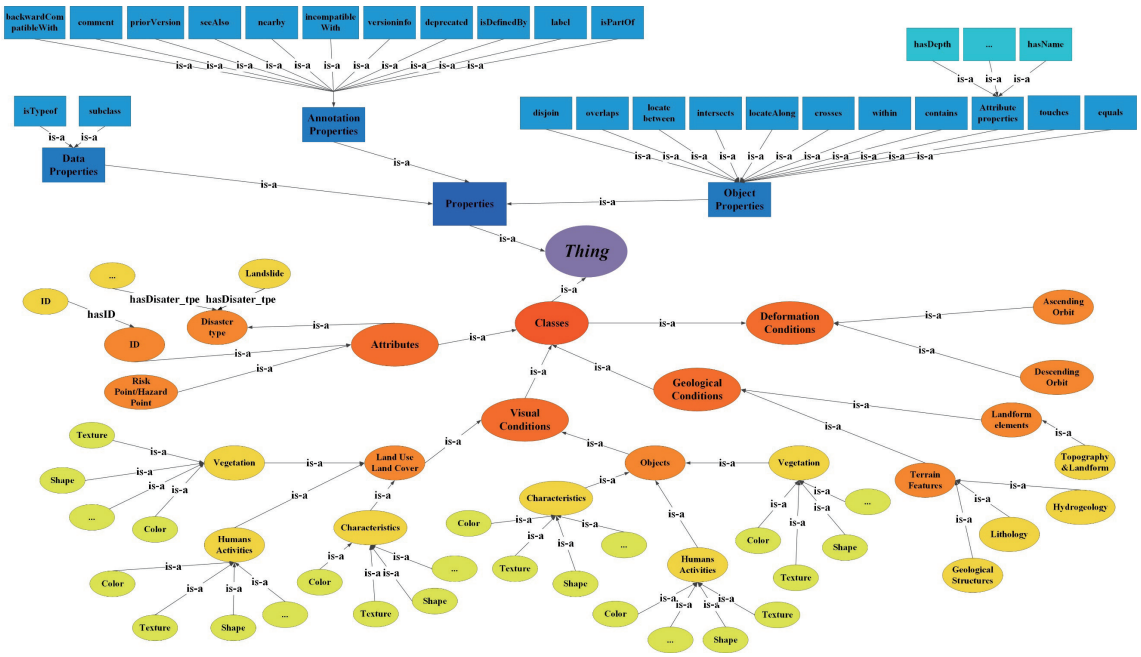

Fig. 3. (Color online) Architecture of developed ontology.

enriched dataset shown in Fig. 1. The Attributes class defines meta-information and basic semantic information that can be used to define landslide/mudslide susceptibility. The Visual Conditions class defines visual interpretation results from optical remote sensing images. It includes two subclasses, namely, Land Use/Land Cover and Object, each of which includes three subclasses (i.e., Vegetation, Human Activities, and Characteristics). It also formally expresses the results from visual features. The Geological Conditions class defines the topographical and terrain features regarding landslide/mudslide susceptibility. It includes two subclasses, namely, Terrain Features and Landform Elements. In addition, the subclasses for Terrain Features and Landform Elements are Geological Structures and Lithology, and Topography & Landform and Hydrogeology, respectively. The Deformation Conditions class includes Ascending Orbit and Descending Orbit, which define the deformation features regarding landslide/mudslide susceptibility.

Property defines the relationship between classes and individuals in the ontology and comprises three mutually exclusive subclasses, namely, Object, Data, and Annotation properties. Object properties express relationships between classes or objects of different classes. For instance, isSubClassOf defines the parent–child relationship between two classes. Data properties are used to define the relationship between an object and a literal data type. The literal data type should conform to either the RDF literal or XML schema data type. As an example, all wavebands have preset wavelength values, so we use a data property of hasWavelength to represent it. The subject of this property is a floating number representing the wavelength value. The third property type, the Annotation property, describes the meta-information of the developed ontology. For instance, priorVersion specifies a parent ontology from which this ontology is extended. The RDF version defines the version of RDF used to encode the ontology. We directly adopted the annotation properties defined by the Resource Description Framework Schema (RDFS) into our ontological development (see Table 2).

All properties and their restrictions defined in the developed ontology are shown in Table 2. These properties not only include those defined at the class level in the conceptual model but also contain the relationships between individuals and classes or between individuals and other individuals. For instance, the triple <A, isInstancesOf, B> expresses that A is a type of B. Here, A can be an object NASA, and B can be the class Provider (data provider). equalsTo expresses

Table 2
Definition of properties and restrictions used in ontology.

Object property	Object restriction	Data property	Data restriction	Annotation property
isSubClassOf, isInstanceOf, equalsTo, hasMetadata, hasCoverage, hasProvider, hasSensor	Some (existential)* Only (universal)* Functional* Inverse functional* Transitive* Symmetric* Asymmetric* Reflexive* Irreflexive*	hasSpatialResolution, hasProminentWaveband, hasWavebandNumber, hasShootingTime, hasWeight, hasPriority isRankedAs hasWavelength, hasReflectance	Some (existential)* Only (universal)* Min (min cardinality)* Exactly (exact cardinality)* Max (max cardinality)* Functional*	isDefinedBy* priorVersion* ontologyLevel applicationField ontologyVersion RDFVersion OWLVersion XMLVrsion SWRLVersion SPARQLVersion ontologyIRI

*Restrictions defined by RDFS and OWL standards.

the "same" relationship between two objects (they could be either classes or individuals). The property hasID is used to define the ID for a landslide/mudslide individual.

Moreover, the spatial coverage, data provider, and sensor information can be linked through properties such as covers, hasProvider, and hasSensor, respectively. In the data property column, hasSpatialResolution and hasShootingTime are used to record the spatial resolution (in meters), the total number of wavebands, and the time that the data is captured. Because the data type of objects for the two properties hasSpatialResolution is structured as Integers, and that for hasShootingTime is a Date, they are all categorized as data properties. Object and data restrictions were also created to set additional restrictions on the object and data properties in a triple. These restrictions were adopted from the W3C OWL standard.

4. Prototype of Semantically Enriched Results

4.1 Triples-based semantic descriptions

The results of data interpretation can be accessed through the link: https://pan.baidu.com/s/1dSw3qXRxtyCBYxewXN01aQ, with the password 03zm. Then, we employed the semantic modeling approaches mentioned in Sect. 3.3 to convert the content in Table 3 into triples.

Table 3
Records of data-based interpretation results.

Category	Interpretation descriptions
ID	0001
Disaster type	Landslide
Risk point/hazard point	Existing Risk Point
Vegetation	The vegetation within the landslide is a tree forest, distributed on the upper side of the landslide.
Human activities	Slope cutting for house construction
Characteristics	The landslide overall appears chair-like, with the landslide body mainly consisting of vegetation and partially rural houses.
Geological structure	A general fault is oriented to the northwest on the right side within the landslide.
Lithology	Within the landslide, there is a distribution of thin-to-medium layered sandstone, muddy sandstone, metamorphic mudstone, silty shale, metamorphic shale, feldspar quartz sandstone, and softer rock groups.
Topography & landform	The landslide is located in a deep cut high-mountain gorge terrain.
Hydrogeology	Bedrock fissure water - weathered belt reticular fissure water - medium water-richness, the modulus of underground runoff is 1–3 liters/second per square kilometer, and the spring flow rate is 0.5–1 liters/second
Ascending orbit	In the ascending track deformation rate diagram, the landslide body undergoes deformation, with the maximum deformation rate of 10.85 mm/year, the minimum deformation rate of 0.05 mm/year, and the average deformation rate of 4.06 mm/year.
Descending orbit	In the descending track deformation rate diagram, the landslide body undergoes deformation, with the maximum deformation rate of 8.68 mm/year, the minimum deformation rate of 0.34 mm/year, and the average deformation rate of 4.78 mm/year.
Triples-based semantic descriptions	The landslide overall appears dustpan-like, with a broken surface and steep terrain, mainly wasteland.
Threats	Residential Area, Agricultural Land
Risk evaluation	Low

Table 3
(Continued) Records of data-based interpretation results.

Category	Semantic triples
ID	hasID 0001
Disaster type	hasDisasterType Landslide
Risk point/hazard point	is-A Existing risk point
Vegetation	hasVegetation tree forest, hasDistributed landslide, isUpperSide landslide
Human activities	hasHumanActivities house construction
Characteristics	hasAppears chair-like, consistOf vegetation, consistOf rural houses (partially)
Geological structure	fault isOrientedTo northwest {isRightSide landslide}
Lithology	hasDistributed thin-to-medium layered sandstone, hasDistributed muddy sandstone, hasDistributed metamorphic mudstone, hasDistributed silty shale, hasDistributed metamorphic shale, hasDistributed feldspar quartz sandstone, hasDistributed softer rock groups
Topography & landform	landslide isLocatedIn high-mountain gorge terrain, high-mountain gorge terrain is-A a deep cut.
Hydrogeology	is-A bedrock fissure water, is-A weathered belt reticular fissure water, is-A medium water-richness, the modulus of underground runoff hasModulus 1-3 spring hasFlowRate 0.5-1
Ascending orbit	landslide undergoes ascendingDeformation, landslide hasMaxDeformationRate 10.85, landslide hasMinDeformationRate 0.05, landslide hasAvgDeformationRate 4.06
Descending orbit	landslide hasDescendingDeformation, landslide hasMaxDeformationRate 8.68, landslide hasMinDeformationRate 0.34, landslide hasAvgDeformationRate 4.78
Triples-based semantic descriptions	landslide hasAppears dustpan-like, landslide hasAppears broken surface, landslide hasAppears steep terrain, consistOf wasteland.
Threats	isThreatenedBy Residential area
Risk evaluation	hasRisk Low

Table 3 illustrates the selected results of interpretation descriptions, and the semantic triples correspond to the descriptions. In the semantic triples part, italic texts, such as hasID and hasDistributed, refer to the relationships in "subject-relationship-object", or the property in "domain-property-range". (*) such as (partially) refers to restriction. Moreover, the words with the first capital character, such as Landslide and Existing risk point, refer to a class name, and the words with no capital characters refer to an individual.

4.2 Logic-reasoning-enhanced semantic query

Before conducting sematic query, we use the Semantic Web Rule Language (SWRL), a Rule Markup language to generate a series of rules to support logical reasoning on top of OWL ontologies.[29] Depending on the full power of OWL, the rules in SWRL are constructed from an "antecedent (body) and consequent (head)" form. This form provides that any conditions satisfied in antecedent are also satisfied in the consequent. The query language is encoded in the semantic web query language SPARQL. Below, we pose three questions, each representing a query type mentioned above to demonstrate the reasoning by the interpretation results.

To test our geospatial semantic model for change information from remote sensing imagery, we designed a series of semantic queries on the basis of the ontological model.

(1) Which landslide susceptibility points are affected by construction in 2022?

The basic SQL language of this query is SELECT "Human Activities" FROM "Landslide" AND "2012". The syntax of SPARQL query is listed in Table 4.

(2) Historical trajectory of the lithology distribution of the landslide susceptibility point with ID 0001 from 2009 to 2012.

The basic SQL language of this query is SELECT "ID" FROM "0001" AND "2012". The syntax of SPARQL query is listed in Table 5.

4.3 Knowledge graph generation

The semantic information in the ontology supports to generate a knowledge graph for land use/land cover domain, which is shown in Fig. 4. To better visualize the structure of the

Table 4
Syntax of SPARQL query.

Item	Details
Standards	rdf: http://www.w3.org/1999/02/22-rdf-syntax-ns# owl: http://www.w3.org/2002/07/owl# xsd: http://www.w3.org/2001/XMLSchema# rdfs: http://www.w3.org/2000/01/rdf-schema# s2cd: http://www.semanticweb.org/ontologies/2023/10/landslide-ontology-1#
Query (SELECT)	?who ?HumanActivities
Conditions (WHERE)	?who <http://www.semanticweb.org/ontologies/2023/10/landslide-ontology-1#hasDisasterType> <http://www.semanticweb.org/ontologies/2023/10/landslide-ontology-1#Landslide>. ?who <http://www.semanticweb.org/ontologies/2023/10/landslide-ontology-1#hasYear> <http://www.semanticweb.org/ontologies/2023/10/landslide-ontology-1#2022>.

Table 5
Syntax of SPARQL query.

Item	Details
Standards	rdf: http://www.w3.org/1999/02/22-rdf-syntax-ns# owl: http://www.w3.org/2002/07/owl# xsd: http://www.w3.org/2001/XMLSchema# rdfs: http://www.w3.org/2000/01/rdf-schema# s2cd: <http://www.semanticweb.org/ontologies/2023/10/landslide-ontology-1#>
Query (SELECT)	?who ?Year ?Lithology ?ID
Conditions (WHERE)	<http://www.semanticweb.org/ontologies/2023/10/landslide-ontology-1#?who. ?who <http://www.semanticweb.org/ontologies/2023/10/landslide-ontology-1#hasYear> ?Year. ?who <http://www.semanticweb.org/ontologies/2023/10/landslide-ontology-1#hasLandUse> ?Lithology. ?who <http://www.semanticweb.org/ontologies/2023/10/landslide-ontology-1#hasID> ?ID. <http://www.semanticweb.org/ontologies/2023/10/landslide-ontology-1#0001>. <http://www.semanticweb.org/ontologies/2023/10/landslide-ontology-1#hasDistributed> ?Lithology. ?who <http://www.semanticweb.org/ontologies/2023/10/landslide-

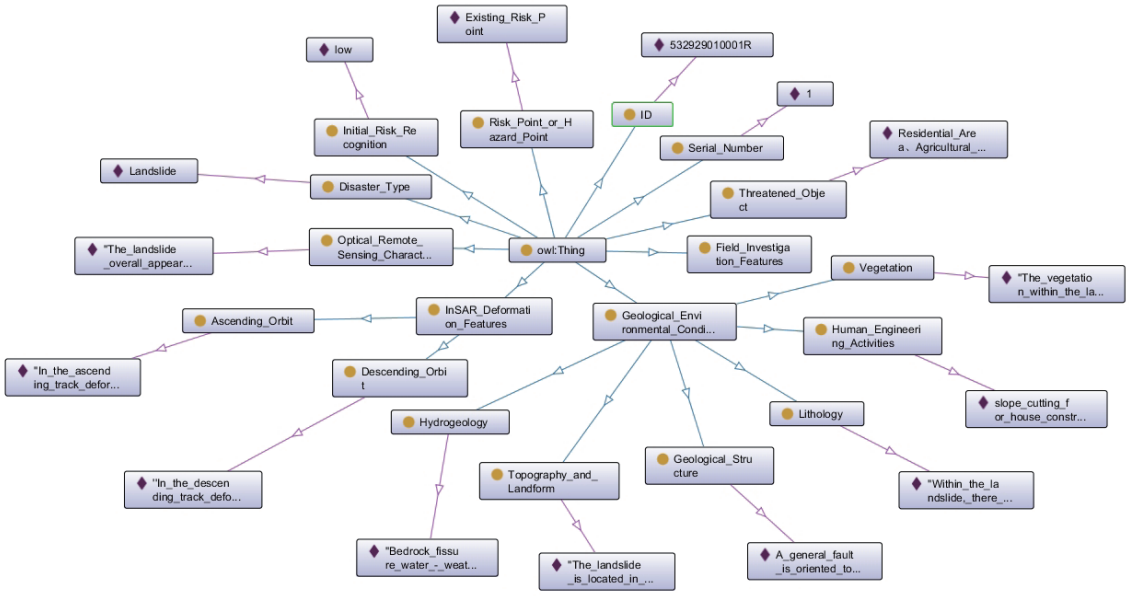

Fig. 4. (Color online) Illustration of knowledge graph generated from the developed ontology (visualized by Protégé).

knowledge graph, we employ Protégé to generate this knowledge graph. Every class and their individuals are annotated by yellow and purple. Moreover, every relationship is also annotated. Since these classes and individuals are organized by semantic triples, all contents included in the generated knowledge graph can be accessed by logic reasoning, updated, and fused with other ontologies.

5. Conclusion

To establish an efficient methodology to model the landslide/mudslide susceptibility and support various hazard monitoring and prediction applications, we developed a spatial ontology to explicitly model the complexity of landslide/mudslide susceptibility. Depending on four major components (property, relation, role, and restriction), the developed ontology can represent the descriptions in terms of landslide/mudslide susceptibility at different levels. This ontological model can also represent the landslide/mudslide susceptibility in terms of multiple facets including visual, deformation, and terrain features. Furthermore, a series of semantic queries based on SPARQL were developed to support the retrieval of dynamic changes of LULC information.

Earlier studies of landslide/mudslide susceptibility modeling lack a knowledge-based approach to connect the result of landslide/mudslide susceptibility with geoinformation in GIS or spatial databases. Our work can integrate multimodal remote sensing information into the proposed ontological model to enhance the space–time analysis of emergency management in a complex manner. Finally, historical trajectories, present conditions, and changes regarding a landslide/mudslide susceptibility point can be accessed on the basis of the set of semantic queries.

As a study to facilitate modeling and semantic query of landslide/mudslide susceptibility, there are several possible extensions of this research. The ontological definition of classes and instances in this work is centered on discrete geospatial objects, and we will extend this ontological model to formally describe the geographical scenes that contain both objects and relationships between objects. Finally, we will integrate this semantic modeling and query framework into a cyberinfrastructure platform to support collaborative querying and decision-making of land use and land cover change.

Acknowledgments

This work was supported by Key Technology Research and Development Program of Shan Dong Provincial Bureau of Geology&Mineral Resources under grant NO. KY202224. Huzhou Key Research and Development Program under grant NO.2023ZD2046, Beijing Nova Program, under grant NO.20230484351, and Open Topic of the Hunan Engineering Research Center of 3D Real Scene Construction and Application Technology under grant NO. 3DRS2024Y1.

References

1 F. Yang, X. Z. Men, Y. S. Liu, H. G. Mao, Y. N. Wang, L. Wang, X. R. Zhou, C. Niu, and X. Xie: Land **12** (2023) 1. https://doi.org/10.3390/land12101949
2 X. Z. Xu, Z. Y. Liu, W. L. Wang, H. W. Zhang, Q. Yan, C. Zhao, and W. Z. Guo: Nat. Hazards **76** (2015) 1939. https://doi.org/10.1007/s11069-014-1570-0
3 C. Zhou, K.L. Yin, Y. Cao, B. Ahmed, Y. Y. Li, F. Catani, and H. R. Pourghasemi: Comput. Geosci. **112** (2018) 23. https://doi.org/10.1016/j.cageo.2017.11.019
4 M. S. Roodposhti, J. Aryal, and B. A. Bryan: Environ. Model. Softw. **112** (2019) 70. http://doi.org/10.1016/j.envsoft.2018.10.006
5 A. Singleton, Z. Li, T. Hoey, and J. P. Muller: Remote Sens. Environ. **147** (2014) 133. https://doi.org/10.1016/j.rse.2014.03.003
6 P. Tizzani, P. Berardino, F. Casu, P. Euillades, M. Manzo, G. P. Ricciardi, G. Zeni, and R. Lanari: Remote Sens. Environ. **108** (2007) 277. https://doi.org/10.1016/j.rse.2006.11.015
7 A. Ferretti, C. Prati, and F. Rocca: IEEE Trans. Geosci. Remote Sens. **39** (2001) 8. https://doi.org/10.1109/36.898661
8 A. Rosi, V. Tofani, L. Tanteri, C.T. Stefanelli, A. Agostini, F. Catani, and N. Casagli: Landslides **15** (2018) 5. https://doi.org/10.1007/s10346-017-0861-4
9 H.J. Cai, T. Chen, R.Q. Niu, and A. Plaza: IEEE J. Sel. Top. Appl. Earth Obs. Remote Sens. **14** (2021) 5235. https://doi.org/10.1109/jstars.2021.3079196
10 Q. Xu, D.L. Peng, S. Zhang, X. Zhu, C. Y. He, X. Qi, K. Y. Zhao, D. H. Xiu, and N. P. Ju: Eng. Geol. **279** (2020) 278. https://doi.org/10.1016/j.enggeo.2020.105817
11 A. Musaev, D. Wang, and C. Pu: IEEE Trans. Serv. Comput. **8** (2015) 715. https://doi.org/10.1109/tsc.2014.2376558
12 M. Polcari, E. Ferrentino, C. Bignami, S. Borgstrom, R. Nappi, and V. Siniscalchi: IEEE J. Sel. Top. Appl. Earth Obs. Remote Sens. **16** (2023) 5686. https://doi.org/10.1109/jstars.2023.3286993
13 F. K.Sufi and M. Alsulami: IEEE Access **9** (2021) 131400. https://doi.org/10.1109/access.2021.3115043
14 J. Barlow, S. Franklin, and Y. Martin: Photogramm. Eng. Remote Sens. **72** (2006) 687. https://doi.org/10.14358/pers.72.6.687
15 J. Iwahashi, I. Kamiya, and H. Yamagishi: Geomorphology **153** (2012) 29. https://doi.org/10.1016/j.geomorph.2012.02.002
16 X. Xie, X. Zhou, B. Xue, Y. Xue, K. Qin, J. Li, and J. Yang: Chin. Geogr. Sci. **31** (2021) 915. https://doi.org/10.1007/s11769-021-1233-5
17 X. R. Zhou, W. W. Li, and S. T. Arundel: Int. J. Geogr. Inf. Sci. **33** (2019) 666. https://doi.org/10.1080/13658816.2018.1554814

18 P. Reichenbach, M. Rossi, B. D. Malamud, M. Mihir, and F. Guzzetti: Earth Sci. Rev. **180** (2018) 60. https://doi.org/10.1016/j.earscirev.2018.03.001
19 M. Scaioni, L. Longoni, V. Melillo, and M. Papini: Remote Sens. **6** (2014) 9600. https://doi.org/10.3390/rs6109600
20 E. V. Marcelino, A. R. Formaggio, and E. E. Maeda: Int. J. Appl. Earth Obs. Geoinf. **11** (2009) 181. https://doi.org/10.1016/j.jag.2009.01.003
21 G. J. Wang, M. Xie, X. Chai, L. W. Wang, and C. X. Dong: Environ. Earth Sci. **69** (2013) 2763. https://doi.org/10.1007/s12665-012-2097-x
22 P. Berardino, G. Fornaro, R. Lanari, and E. Sansosti: IEEE Trans. Geosci. Remote Sens. **40** (2002) 2375. https://doi.org/10.1109/tgrs.2002.803792
23 R. Lanari, O. Mora, M. Manunta, J. J. Mallorquí, P. Berardino, and E. Sansosti: IEEE Trans. Geosci. Remote Sens. **42** (2004) 1377. https://doi.org/10.1109/tgrs.2004.828196
24 S. Li, W. Xu, and Z. Li: Geod. Geodyn. **13** (2022) 114. https://doi.org/10.1016/j.geog.2021.09.007
25 L. L. Zhang, K. R. Dai, J. Deng, D. Q. Ge, R. B. Liang, W. L. Li, and Q. Xu: Remote Sens. **13** (2021) 3662. https://doi.org/10.3390/rs13183662
26 X. Liu, C. Zhao, Q. Zhang, Z. Lu, Z. Li, C. S. Yang, W. Zhu, J. Liu-Zeng, L. Q. Chen, and C. J. Liu: Eng. Geol. **284** (2021) 106033. https://doi.org/10.1016/j.enggeo.2021.106033
27 M. Kavouras and M. Kokla: The SAGE Handbook of GIS and Society (SAGE, 2011) pp. 46–66. https://doi.org/10.4135/9781446201046.n3
28 A. R. D. Prasad and N. Guha: Online Inf. Rev. **32** (2008) 500. https://doi.org/10.1108/14684520810897377
29 I. Horrocks, P. F. Patel-Schneider, S. Bechhofer, and D. Tsarkov: J. Web Semant. **3** (2005) 23. https://doi.org/10.1016/j.websem.2005.05.003